

Characterising Electron Transfer Mechanism in Tribo-Electrification of Pyrite Through Contact Angle Measurements

R. K. Dwari* and K. Hanumantha Rao*

Division of Mineral Processing, Luleå University of Technology, SE-971 87 LULEÅ, Sweden

Abstract: Coal beneficiation by tribo-electrostatic method depends on tribo-charging attributes of coal and ash forming minerals. The tribo-electrification behaviour of pyrite mineral contacted with different materials has been investigated through charge measurements and the charge acquisition is probed through surface energy calculations from liquid contact angle data. Liquid contact angle on pyrite powder after tribo-electrification is determined by Krüss tensiometer using Washburn's equation. The sample holder in tensiometer is specially fabricated with different materials serving the purpose of tribo-electrification and contact angle measurement. The acid and base parameters of pyrite surface determined with van Oss acid-base approach using liquid contact angle data after tribo-electrification with different materials revealed the charging phenomena and electron transfer mechanism. The results showed an explicit correlation between the charge generated by pyrite powder and surface acceptor (acid)-donor (base) electronic state underlying the work functions of contacting surfaces. Thus a method for characterising the changes in surface energetic structure of solids during contact electrification in terms of surface acid-base parameters has been illustrated for the first time.

INTRODUCTION

Coal is the single largest fossil energy source used worldwide and accounts for more than 60% of the total commercial energy consumed. The major portion of the coal used for such power generation is not clean enough to maintain the rigorous environmental standards required these days world over. The problem is the high sulphur content in coal used in most of the western countries or ash as is the case in countries like India. The sulphur content in coals globally varies from 0.38 to 9% and rarely exceeds this range. The sulphur content in non-coking coals of India is generally below 0.5% and mostly in the form of pyrite. However, the North-Eastern coals contain 2-7% sulphur and about 75-90% of this sulphur is organic in nature [1]. Coals in the Western countries also contain pyritic sulphur and removal of this sulphur alone could reduce the total sulphur content to less than 1%, well below the pollution control standard. Electrostatic separator with tribo-charging technique has great potential for the separation of pyrite from coal in fine size materials, but organic sulphur is not accessible to this dry physical separation technique as it is covalently bound with carbon in macerals [2]. There have been some investigations carried out using tribo-electrostatic method but has not achieved commercial status in coal beneficiation industry.

The tribo- or contact electrification of materials is a well-known effect, which is a function of the ability of material to accept or donate electrons when it is in dynamic contact with other material. The net charge acquisition by the material in tribo-electrification depends on the work function difference between the contacting materials. In recent years, there has been a broad understanding that electron transfer during contact charging is due to surface properties rather than bulk

properties of materials and the amount and polarity of charge transfer between two dissimilar materials is controlled partly by their surface chemistry. The ability of particles to donate or accept electrons is an inherent property of particles based on their work function and physical form and it is logical to believe that there must be an underlying tendency for a material to charge, which is a consequence of its surface energetic electron donating/electron accepting properties. Accordingly, contact electrification is also explained as acid-base interactions between surfaces involving protons in the case of Brönsted acids-bases or electrons in the case of Lewis acids-bases. The acid-base interactions associate charge rearrangement at the interface and, when the interacting surfaces are abruptly separated, some fraction of charge may remain on the surface. The surface acidity and basicity are thus related to surface acceptor and donor electronic states and thereby to work functions. The work functions of metals can be easily determined reliably but they are not established for insulating materials. The published work function values for the same material varied because of different surface states caused by impurities, crystal imperfections, defects, etc. Despite the fact that the surface physico-chemical properties will influence the extent of charging, characterization of surface energetic electron donating/accepting properties before and after contact charging has not been illustrated till today, primarily due to the lack of standard instrumentation and procedures. Many authors quantified the acid-base character of mineral surfaces by solvatochemistry [3], zeta-potential [4], inverse gas chromatography (IGC) [5], liquid contact angles [6,7], etc. In the context of triboelectrification, electron donating-accepting tendencies of pharmaceutical powders have been investigated by IGC and obtained a correlation between the charges generated in tribo-electric studies of powders and acid/base parameters determined by the IGC. However, no studies have been reported up today on the characterisation of electron transfer emphasising the changes

*Address correspondence to these authors at the Luleå University of Technology, Luleå, Sweden; Fax: +46 920 973 64; Tel: +46 920491712 (O); E-mail: ranjan.dwari@ltu.se, Hanumantha.Rao@ltu.se

in surface acid-base properties of contacting surfaces before and after tribo-electrification.

The pyritic sulphur could be in the form of pyrite and marcasite. Both pyrite and marcasite have similar chemical composition but possess different crystalline forms of cubic and orthorhombic respectively. Pyrite is the most commonly reported mineral while marcasite has often been mentioned as occurring in lesser amount except in Victorian brown coal of Australia, where it is the only sulphide mineral. According to Esposito *et al.* [8], there is a difference in the properties of coal pyrite and ore pyrite in terms of morphology, specific gravity and surface area. A detailed understanding of the surface properties of pyrite after tribo-charging with different materials is necessary for an efficient rejection of pyrite from coal. The aim of the present work is, therefore, to understand and quantify the surface energetic structure of pyrite, which is one of the most important ash-forming minerals in coal in terms of acidity and/or basicity, before and after tribo-electrification with different materials, and thereby to identify the optimum tribo-charger material in dry coal beneficiation. In the present investigations, tribo-electrification of pyrite and electron transfer between the two contacting materials in terms of surface acid-base properties were studied using glass, copper, aluminium and brass as tribo-charging media. Investigations on marcasite and coal pyrite will be considered in a future work.

THEORY

The surface free energy and interfacial free energy of solids are extremely useful in predicting material processes and properties. The problem of experimental determination and theoretical calculations of solid surface free energy is still open. Nevertheless, several approaches have been reported in literature, which makes it possible to evaluate solids surface energy using contact angle data of liquids with known surface energy parameters. The first approach is that of Zisman [9], which defines that the surface energy of a solid is equal to the surface tension of the highest surface tension liquid that will completely wet the solid, i.e., zero contact-angle. This comes from the widely observed tendency of contact angle on a solid surface to decrease as liquid surface tension decreases. During later years, the following approaches have been described to determine the surface energy through liquid contact angles on solid surfaces:

FOWKES APPROACH

The most widely used two components surface energy theory is due to Fowkes [10-12]. It suggests that the surface energy of a solid is a summation of two components, viz. a dispersive component and a non-dispersive or polar component. The dispersive component theoretically accounts for van der Waals and non-site specific interactions that a surface is capable of having with applied liquids. The polar component is accounted for dipole-dipole, dipole-induced dipole, hydrogen bonding, and other site-specific interactions, which a surface is capable of having with applied liquids. The approach is based on three fundamental equations, which describe interactions between solid surfaces and liquids. These equations are:

Young's equation

$$\gamma_s = \gamma_{sl} + \gamma_l \cos \theta \quad \dots (1)$$

where γ_s = overall surface energy of the solid, γ_l = overall surface tension of the wetting liquid, γ_{sl} = the interfacial tension between the solid and the liquid and θ = the contact angle between the liquid and solid.

Dupre's definition of adhesion energy is

$$I_{sl} = \gamma_s + \gamma_l - \gamma_{sl} \quad \dots (2)$$

where I_{sl} = energy of adhesion per unit area between a liquid and a solid surface.

Fowkes' theory assumes that the adhesive energy between a solid and a liquid can be separated into interactions between the dispersive components of the two phases and interactions between the non-dispersive (polar) components of the two phases:

$$I_{sl} = 2 \left[\left(\gamma_l^D \right)^{1/2} \left(\gamma_s^D \right)^{1/2} + \left(\gamma_l^P \right)^{1/2} \left(\gamma_s^P \right)^{1/2} \right] \quad \dots (3)$$

where γ_l^D = dispersive component of the surface tension of the wetting liquid, γ_s^D = dispersive component of the surface energy of the solid, γ_l^P = polar component of the surface tension of the wetting liquid, and γ_s^P = polar component of the surface energy of the solid.

The above three equations are combined to yield the primary equation of the Fowkes' surface energy theory.

$$\left(\gamma_s^D \gamma_l^D \right)^{1/2} + \left(\gamma_s^P \gamma_l^P \right)^{1/2} = \frac{\gamma_l (1 + \cos \theta)}{2} \quad \dots (4)$$

Since the above equation has two unknowns, γ_s^D and γ_s^P , the contact angle data from two well characterised polar and apolar liquids are needed.

VAN OSS ACID-BASE APPROACH

van Oss [13-15] and his associates were the first to calculate the surface energy of solid as the addition of Lifshitz-van der Waals (γ^{LW}) and polar or Lewis acid-base (γ^{AB}) interaction given by the equation

$$\gamma = \gamma^{LW} + \gamma^{AB} \quad \dots (5)$$

Apolar interaction or the Lifshitz-van der Waals component of surface energy results from dispersion (London's force), induced dipole-dipole (Debye's force) and dipole-dipole (Keesome's force) intermolecular interactions. Lewis acid-base (γ^{AB}) or polar interactions are due to hydrogen bonding interactions (acid-base) and most generally electron acceptor, γ^+ , and electron donor, γ^- , interactions. The component γ^{AB} is expressed as the geometric mean of γ^+ and γ^- , and is given by

$$\gamma^{AB} = 2 \left(\gamma^+ \gamma^- \right)^{1/2} \quad \dots (6)$$

The solid-liquid interfacial free energy is expressed as follows:

$$\gamma_{sl}^{LW} = \left[\left(\gamma_s^{LW} \right)^{1/2} - \left(\gamma_l^{LW} \right)^{1/2} \right]^2 \quad \dots (7)$$

$$\gamma_{sl}^{AB} = 2 \left[\left(\gamma_s^+ \gamma_s^- \right)^{1/2} + \left(\gamma_l^+ \gamma_l^- \right)^{1/2} - \left(\gamma_s^+ \gamma_l^- \right)^{1/2} - \left(\gamma_l^+ \gamma_s^- \right)^{1/2} \right] \dots (8)$$

Combining equations 7 and 8, the total free surface energy can be expressed as

$$\gamma_{sl}^{Total} = \left[\left(\gamma_s^{LW} \right)^{1/2} - \left(\gamma_l^{LW} \right)^{1/2} \right]^2 + 2 \left[\left(\gamma_s^+ \gamma_s^- \right)^{1/2} + \left(\gamma_l^+ \gamma_l^- \right)^{1/2} - \left(\gamma_s^+ \gamma_l^- \right)^{1/2} - \left(\gamma_l^+ \gamma_s^- \right)^{1/2} \right] \quad \dots (9)$$

Combining the above equation with Young's equation, the following relation is obtained:

$$(1 + \cos \theta) \gamma_l = 2 \left[\left(\gamma_s^{LW} \gamma_l^{LW} \right)^{1/2} + \left(\gamma_s^+ \gamma_l^- \right)^{1/2} + \left(\gamma_l^+ \gamma_s^- \right)^{1/2} \right] \dots (10)$$

The above equation contains three unknown parameters, viz., γ_s^{LW} , γ_s^+ and γ_s^- , and thus requires contact angle data for three liquids two of which must be polar. The contact angles of water, formamide and 1-bromonaphthalene on pyrite powder are used for the calculation of total surface free energy, polar and non-polar contribution to surface energy, and polar component divided into acid and base parts of surface energy.

EXPERIMENTAL

Materials

Pure crystalline pyrite sample used in the present study was obtained from Gregory Bottley & Lloyd, UK. The min-

eral was crushed and ground in jaw crusher and ball mill respectively and classified into -425+150, -150+38 and -38 μm size fractions. The BET surface area determined for these samples was 0.0588, 0.2161 and 1.1364 m^2g^{-1} respectively. These three size fractions were used for contact charging and contact angle measurements. The particle size distribution of these size fractions was carried out with CILAS particle size analyzer. Standard polar liquids of water and formamide and apolar liquids of n-hexane and 1-bromonaphthalene were used to measure the contact angles on pyrite powders before and after tribo-electrification. The surface energy parameters of these standard liquids are presented in Table 1.

TRIBO-ELECTRIFICATION AND CHARGE MEASUREMENT

The effect of tribo-charger material on charge acquisition by pyrite was studied using cylindrical sample holders made

up of different materials, viz. copper, brass, aluminium and glass. The length and diameter of sample holder were 0.051 m and 0.007 m respectively. One gram of mineral particles is tribo-charged for 40 sec and after contact charging the particles' charge polarity and magnitude were measured by Faraday cup connected to Keithley electrometer.

DYNAMIC CONTACT ANGLE MEASUREMENT

The pyrite powder surface accepts or donates electrons to the tribo-charger material during contact electrification based on their work functions, which eventually increase or decrease the Lewis acid (electron acceptor) or base (electron donor) properties of the powder. Therefore, if a change in surface acid-base properties of the solids can be measured immediately after contact electrification, the charge transfer mechanism between the two contacting surfaces in tribo-electrification can be characterised. The Washburn [16] method was used to determine the liquid contact angle on powders. Essentially, the Washburn equation defines the liquid flow through a capillary and it is given as

Table 1. Physico-Chemical Properties of Test Liquids Used as Absorbents for Capillary Constant and Contact Angle Measurements

Liquid	Density, g/cm^3	Viscosity, mPa.s	Surface Tension, mJ/m^2	Disperse Part, mJ/m^2	Polar Part, mJ/m^2	Acid Part, mJ/m^2	Base Part, mJ/m^2
n-hexane	0.661	0.326	18.4	18.4	0	0	0
Water	0.998	1.002	72.8	21.8	51.0	25.5	25.5
Formamide	1.133	3.607	58.0	39.0	19.0	2.3	39.6
1-Bromo Naphthalene	1.483	5.107	44.4	44.4	0	0	0

$$\frac{m^2}{t} = \frac{c \cdot \rho^2 \cdot \gamma_L \cdot \cos \theta}{\eta} \quad \dots (11)$$

where m is the mass of the penetrating liquid, γ_L is the surface tension of the liquid, ρ is the density of measuring liquid, η is the viscosity of liquid, t is the time, θ is the contact angle and c is a material constant which is dependent on the porous structure of the packed solid particles. In the above equation, γ_L , ρ and η are constants. The mass of penetrating liquid, which rises into the porous packed bed can be monitored as a function of time and t versus m^2 can be plotted. The contact angle of the liquid on the solid, θ , and the solid material constant, c , are the two unknown parameters in the equation. If a Washburn experiment is performed with a liquid which is known to have contact angle of $\theta = 0^\circ$ ($\cos \theta = 1$) on the solid, then the solid material constant is the only remaining unknown in the equation and can thus be determined. Therefore, the constant c is determined with an extra measurement before the first real measurement by using a non-polar liquid like n-hexane with low surface tension (18.4 mJ/m^2), which wets the surface completely.

The Krüss K100 tensiometer was used for determining the liquid contact angle on powder samples according to Washburn method. The powder to be measured was filled into the glass tube sample holder with a filter paper base and suspended from the balance. The filter paper prevents the powder from leaking out through the bottom of the cell. The probe liquid is kept in a glass container mounted on a platform below the powder sample holder, which can move in vertical direction, up and down, by giving necessary command to the Labdesk 3.1 software. After the powder sample bed contacted test liquid, the speed at which liquid rises through powder bed was measured in terms of increase in mass as a function of time. The contact angle, θ , was then calculated using Washburn's equation. The tube sample holder used in the analytical system became convenient for tribo-charging the mineral powder before measuring the contact angle. In the present investigation a known amount of weighed powder was taken into the sample vessel and the powder was tribo-charged by intimately contacting the walls of the sample holder for fixed time. After tribo-charging, the vessel was suspended from the balance for contact angle measurement. Copper, brass and aluminium sample holders were fabricated locally with the same dimensions as those of the glass sample holder of Krüss tensiometer as shown in Fig. (1). The length and inside diameter of sample holders were 0.051 m and 0.007 m respectively. Using these sample holders, the effect of tribo-charging on the sorption of probe liquid and thereby the contact angles of pyrite sample was studied.

Surface energy measurement of powder sample was a two-step technique, viz. capillary constant and contact angle measurement. One gram of mineral powder was weighed and introduced into the sample vessel against fritted filter and tapped 10 times for uniform packing and with practice reproducible packing was achieved for each successive

experiment. After tapping, the sample vessel was suspended to the balance of tensiometer and allowed to touch the surface of a 25 ml n-hexane liquid for packing factor or capillary constant measurement. The capillary constant was measured 4 to 5 times and an average value has been used to determine the contact angle of liquid on mineral powder following the same procedure. The contact angle on pyrite mineral after contact electrification was studied similarly by using glass, copper, brass and aluminium sample holders. In this case the sample holder tube was covered on both sides with plates of the same material of diameter 0.007 m as shown in Fig. (1) and tribo-charged by shaking continuously for 40 sec. Each experiment was performed 4 to 5 times and reproducible results were obtained. The capillary constant measured after tribo-electrification with individual material was used for contact angle measurements with that material. The metal tube sample holder was thoroughly cleaned with deionised water, dried and polished with sand paper after each experiment to avoid any contamination of the metal surface due to oxidation or test liquids.

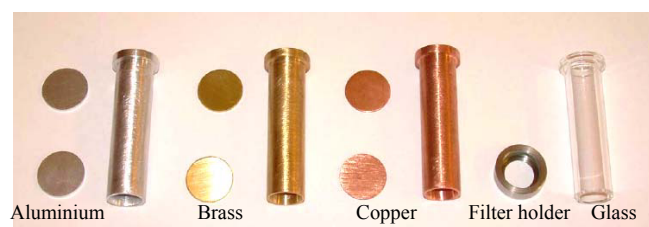


Fig. (1). Sample holder made up of aluminium, brass, copper and glass.

After determining the contact angle of test liquids on pyrite powder, the total surface energy, the polar and non-polar components of surface energy and the division of polar component into acid and base components of surface energy were determined following the theoretical approaches presented above.

RESULTS AND DISCUSSION

Tribo-Electric Studies

The size distribution of different size fractions of pyrite particles are shown in Fig. (2) and the mean diameters of $-425+150$, $-150+38$ and $-38 \mu\text{m}$ size fractions were 248, 98 and $20 \mu\text{m}$, and the BET surface areas were 0.0588, 0.2161 and $1.1364 \text{ m}^2\text{g}^{-1}$, respectively. The charge acquisition of these size fractions of pyrite mineral after contact electrification with different tribo-charging media, viz. glass, brass, Al and Cu was studied. These results shown in Figs. (3) and (4) are presented in terms of unit mass (μCg^{-1}) and unit area (μCm^{-2}) respectively. It can be seen from Fig. (3) that pyrite particles are charged negatively after tribo-electrification with different materials and the results are in very good agreement with reported work functions of Al, 4.28 eV [17], brass, 4.28 eV [18] and Cu, 4.38 eV [19]. Glass has lower work function in tribo-electric series [20] and the increasing order of work function tribo-charging medium is glass, aluminium, brass and copper. The tribo-charge measurements after electrification revealed that pyrite particles charged negatively which means that pyrite has higher work function than the charging medium. The greater

is the work function difference between pyrite and tribo-charger material, the higher is the charge acquisition. Therefore pyrite acquired higher charge and charge density after contact electrification with glass.

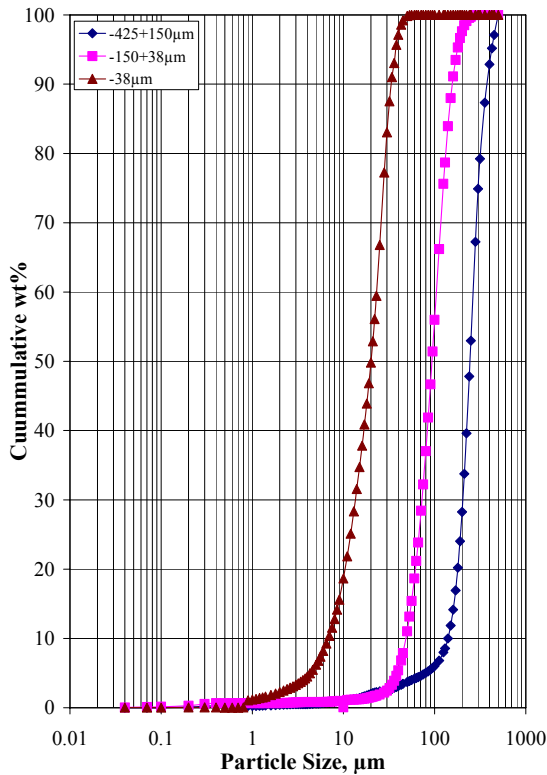


Fig. (2). Particle size distributions of different pyrite size fractions.

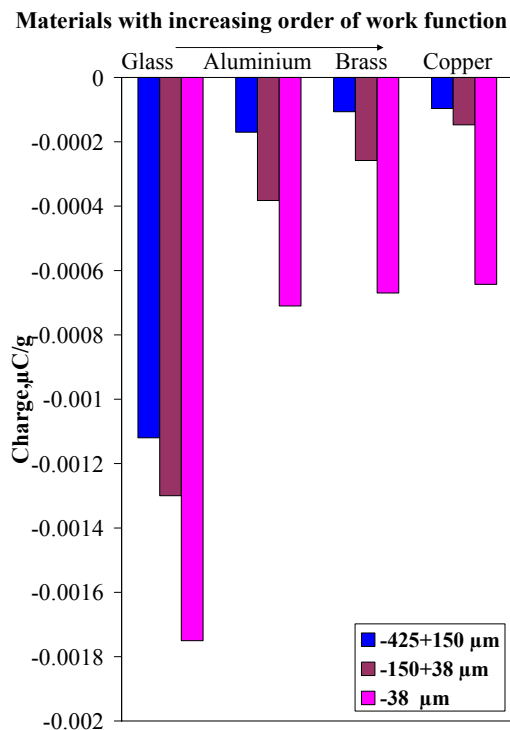


Fig. (3). Effect of tribo-charging on the charge acquisition of different pyrite fractions in μCg^{-1} .

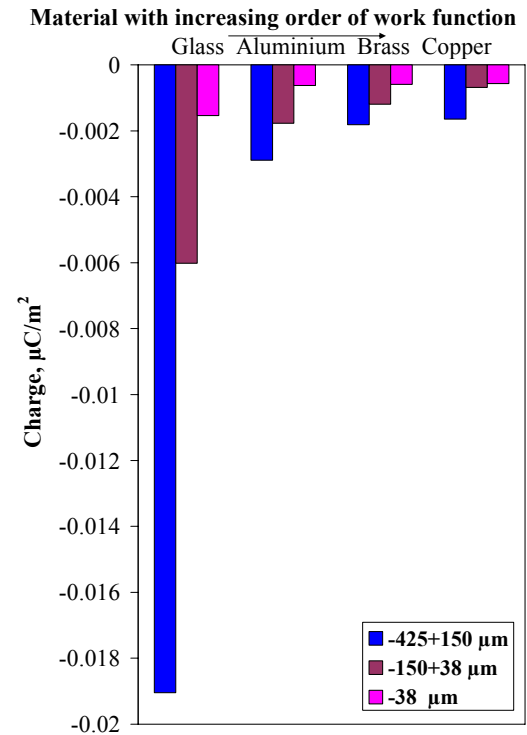


Fig. (4). Effect of tribo-charging on the charge acquisition of different pyrite fractions in μCm^{-2} .

The magnitude of charge acquired per gram of $-38 \mu\text{m}$ pyrite particles is greater than that of the coarser particles because of the higher surface area of fine particles. When charge was analysed in terms of unit area, the magnitude of charge acquired increased in the order -38 , $-150+38$ and $-425+150 \mu\text{m}$ size fractions. This is due to the same tribo-electrification time allowed for charge development for different size fractions of particles. The particles were tribo-charged by shaking in the powder sample holder for 40 sec and this time is not enough for all the particles in finer fraction to have contact with the charging medium for contact electrification. Therefore the magnitude of charge acquired per unit area is less for finer particles than for coarser particles. In order to identify the effect of time on charge acquisition by different size fractions, an experiment has been carried out with copper tribo-charging medium and the results are presented in Fig. (5). In general, the results show that with increasing tribo-charging time the charge ($\mu\text{C}/\text{m}^2$) is increasing for all size fractions of -38 , $-150+38$ and $-425+150 \mu\text{m}$. The results for $-150+38 \mu\text{m}$ size fraction present a limiting equilibrium charge at 40 s time, which charge equals to the charge for the coarser size fraction at 60 s. There is a disturbance during charge measurements for the $-150+38 \mu\text{m}$ size fraction where the charge is less negative at 15 s time compared to the other two size fractions. Nonetheless the results display that the time required for equilibrium charge development for the coarser size fractions is about 40 to 60 s and for the fine $-38 \mu\text{m}$ size fraction more contact electrification time is needed.

EFFECT OF T RIBO-CHARGING ON T HE CAP-ILLARY CONSTANT

As elaborated in the experimental section, the determination of material constant or capillary constant of

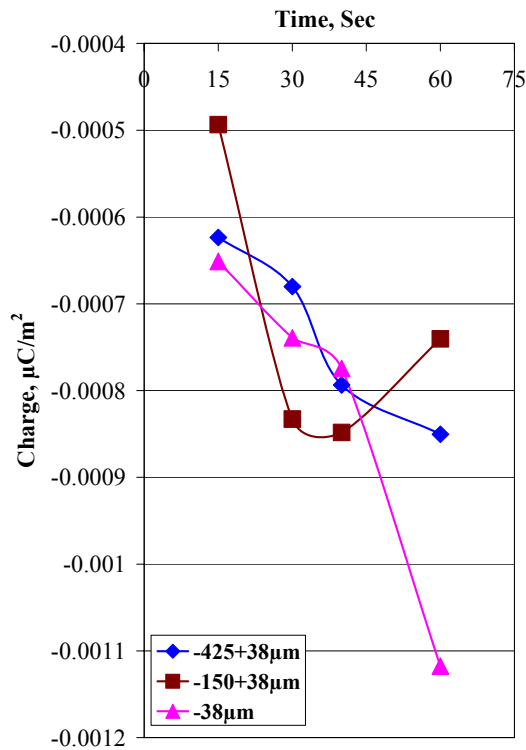


Fig. (5). Effect of time on the charge acquisition on pyrite particles during contact electrification with copper.

powder bed in the sample holder is a prerequisite for measuring the contact angle with different test liquids. Therefore the capillary constants for the three size fractions were measured after tribo-charging with glass, Al, brass and Cu media using n-hexane non-polar liquid having very low surface energy (18.4 mJ/m²) wetting the surface completely. The results are shown in Figs. (6) and (7). The results of capillary penetration experiment of n-hexane through -38 µm pyrite powder bed shown in Fig. (6) was repeated several times so as to ascertain the reproducibility of the result. The results with copper and glass show a good reproducibility

and the curves display the same rate of sorption in a particular sample holder. Although the results with brass and aluminium sample holders are not presented, the n-hexane sorption curves found to be similar with repeated experiments. The capillary constants for the three pyritic size-fractions after tribo-charging with glass, Al, brass and Cu are compared in Fig. (7). It can be seen from this figure that the capillary constant decreases from coarser to finer fraction and increases in the order glass, Al, brass and Cu, which corroborates with increasing order of work function of these materials. The pyrite particles acquired different magnitude of charge and charge density depending on the tribo-charger medium and accordingly the porous structure of packed solids could be different. Higher charge density on the surface leads to strong dipolar character of particles with reference to tribo-charger medium and thereby the particles come closer to each other explaining smaller capillaries and hence lower capillary constant and lower sorption rate. The results are in good agreement with the order of work function values of charging media as well as the size of particles.

EFFECT OF TRIBO-CHARGING ON CONTACT ANGLE

The results on the effect of tribo-charging medium on contact angles of -425+150, -150+38 and -38 µm pyrite size fractions with different test liquids are given in Tables 2, 3 and 4 respectively. The mean contact angle from different runs of a test liquid is presented in these tables. For example, the contact angles calculated for -38 µm pyrite with water as polar test liquid in glass sample vessel are 39.13°, 40.58°, 43.2°, 40.55°, in Al sample vessel are 53.61°, 59.26°, 59.19°, 59.67°, in brass sample vessel are 67.78°, 60.78°, 58.76°, 60.74° and in copper sample vessel are 66.33°, 67.51°, 64.85°, 65.29°. These values show the consistency in the measurements and good reproducibility of results. It can be seen from these tables that the increase in water contact angle follows the increase in the work function order of materials viz., glass, Al, brass and Cu. This trend is consistent with the charge acquisition results. Moreno-Villa *et al.* [21] reported that after exposing porcelain and glass

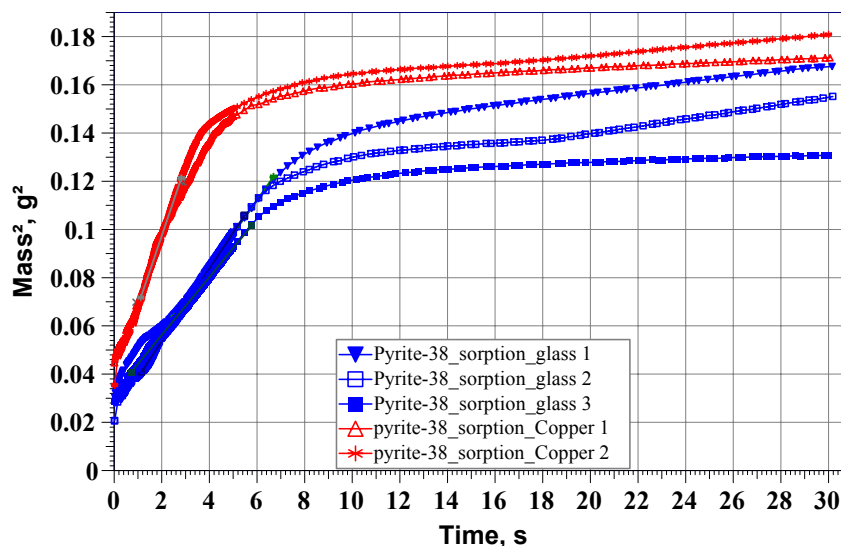


Fig. (6). Effect of tribo-charging on absorption of n-hexane for determining the capillary constant.

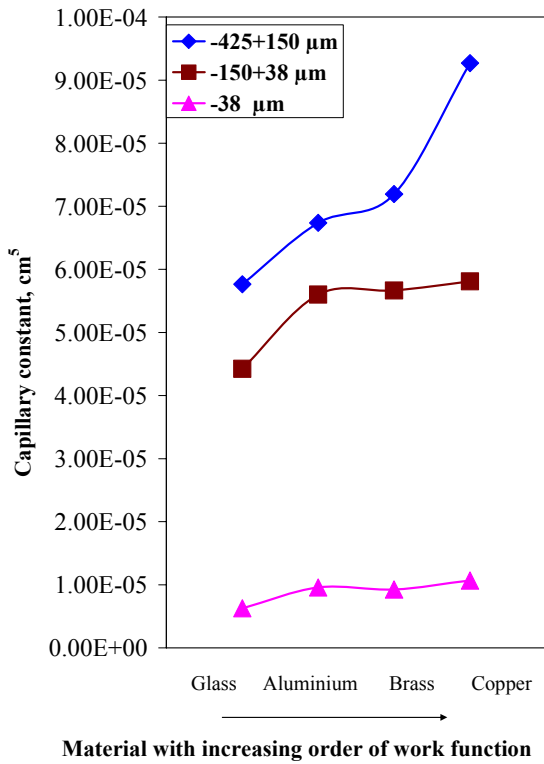


Fig. (7). Effect of tribo-charging on the capillary constant of different size fractions of pyrite.

samples to corona impingement the hydrophobic surface became completely hydrophilic. The same has been observed in the present studies. After contact electrification, the pyrite samples are negatively charged and higher magnitude of charge density is observed with lower work function tribo-charger material. Higher charge accumulation on particle surfaces cause stronger interaction with water and the particle becomes hydrophilic and therefore lower contact angle is observed after contact with glass charging medium. A typical increase in water sorption after tribo-electrification of -425+150 and -150+38 μm pyrite size fractions can be seen in Figs. (8) and (9). The sequence of decreasing contact angles followed the charge acquisition suggesting a correlation between surface charge and wettability of pyrite particles.

SURFACE ENERGY STRUCTURE OF PYRITE AFTER TRIBO-CHARGING

The change in surface characteristics of pyrite after tribo-charging with glass, Al, brass and Cu charging media was assessed by evaluating the surface energy from contact angle data of polar and non-polar test liquids. The Fowkes [10-12] and van Oss acid-base [13-15] approaches were followed for calculating the surface energy of solids. The Fowkes approach calculates the polar and non-polar dispersive components of surface energy. In this case contact angles with two test liquids are required and the dispersive part was first calculated using 1-bromonaphthalene contact angle and then the polar part with water contact angle. The total surface

Table 2. Contact Angle of Test Liquids on - 425+150 μm Pyrite Particles After Contact Electrification with Different Sample Holder Charging Medium

Sample Holder	Capillary Constant, C, cm ⁵	Test Liquids	Contact Angle, in Degrees
Glass	5.7637E-5	n-hexane	0
		Water	49.72±2.53
		Formamide	25.03±1.22
		1-Bromonaphthalene	4.54±0.82
Aluminium	6.7364E-5	n-hexane	0
		Water	56.21±3.78
		Formamide	27.165±2.23
		1-Bromonaphthalene	5.31±0.58
Brass	7.1925E-5	n-hexane	0
		Water	56.98±3.26
		Formamide	30.99±2.72
		1-Bromonaphthalene	22.26±2.73
Copper	9.2692E-5	n-hexane	0
		Water	72.59±3.35
		Formamide	38.1±0.1
		1-Bromonaphthalene	31.89±1

Table 3. Contact Angle of Test Liquids on -150+38 μm Pyrite Particles After Contact Electrification with Different Sample Holder Charging Medium

Sample Holder	Capillary Constant, C, cm^5	Test Liquids	Contact Angle, in Degrees
Glass	4.4235E-5	n-hexane	0
		Water	31.57 \pm 1.93
		Formamide	2.21 \pm 0.49
		1-Bromonaphthalene	4.34 \pm 0.64
Aluminium	5.6009E-5	n-hexane	0
		Water	36.70 \pm 1.75
		Formamide	3.94 \pm 0.51
		1-Bromonaphthalene	4.5 \pm 0.28
Brass	5.6643E-5	n-hexane	0
		Water	42.67 \pm 2.54
		Formamide	6.33 \pm 0.42
		1-Bromonaphthalene	5.37 \pm 0.91
Copper	5.8101E-5	n-hexane	0
		Water	45.48 \pm 3.65
		Formamide	5.72 \pm 0.37
		1-Bromonaphthalene	6.13 \pm 0.85

Table 4. Contact Angle of Test Liquids on - 38 μm Pyrite Particles After Contact Electrification with Different Sample Holder Charging Medium

Sample Holder	Capillary Constant, C, cm^5	Test Liquids	Contact Angle, in Degrees
Glass	6.2667E-6	n-hexane	0
		Water	40.86 \pm 2.34
		Formamide	5.44 \pm 1.57
		1-Bromonaphthalene	5.92
Aluminium	9.5716E-6	n-hexane	0
		Water	57.93 \pm 1.74
		Formamide	4.80 \pm 0.41
		1-Bromonaphthalene	5.35 \pm 0.16
Brass	9.2641E-6	n-hexane	0
		Water	62.01
		Formamide	6.23 \pm 0.37
		1-Bromonaphthalene	6.17 \pm 0.56
Copper	1.0686E-5	n-hexane	0
		Water	65.99 \pm 0.34
		Formamide	5.66 \pm 0.18
		1-Bromonaphthalene	5.62 \pm 0.33

energies and polar and non-polar components of surface energy after tribo-charging with glass, Al, brass and Cu for -425+150, -150+38 and -38 μm particles are given in

Table 5. It can be seen that the total surface energy of 60.60 mJ/m^2 for -425+150 μm pyrite size fraction is higher after tribo-charging with glass in comparison to the surface energy

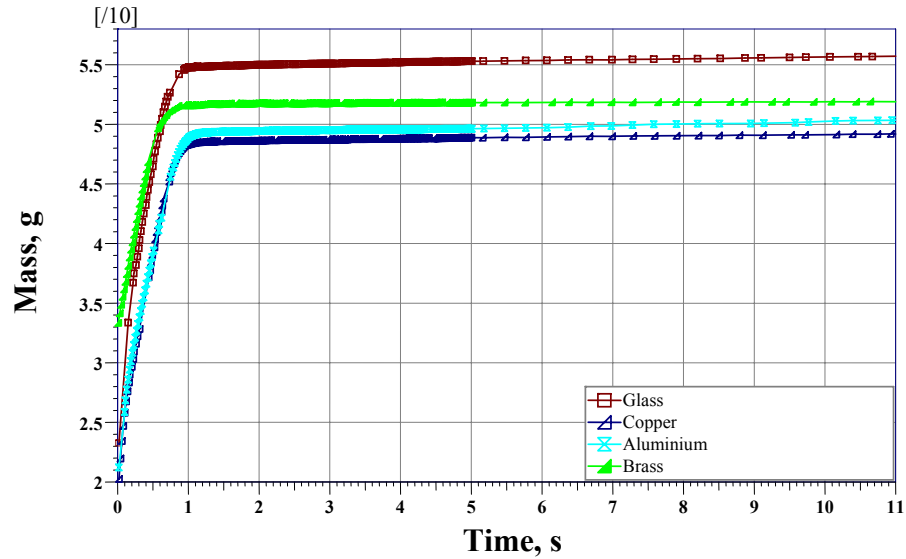


Fig. (8). Effect of tribo-charging on the sorption of water on $-425+150 \mu\text{m}$ pyrite particles during contact angle measurements.

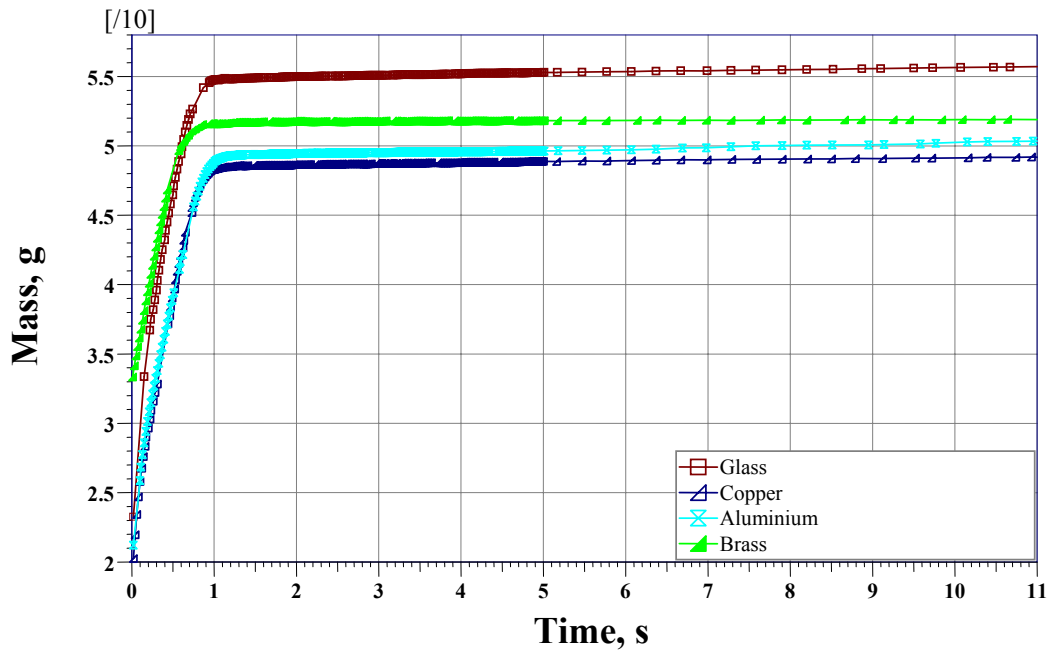


Fig. (9). Effect of tribo-charging on the sorption of water on $-150+38 \mu\text{m}$ pyrite fraction during contact angle measurements.

with aluminium, 57.06 mJ/m^2 , brass, 54.70 mJ/m^2 and Cu, 44.68 mJ/m^2 . The dispersive component value calculated for $-150+38$ and $-38 \mu\text{m}$ is the same after tribo-charging with all the media except for $-425+150 \mu\text{m}$ fraction where dispersive component is lower in case of brass and Cu. In all the three size fractions the polar component is decreasing with increasing order of work function of charging medium. The sequence of surface energy for a particular size fraction followed the increasing order of work function of charging medium and decreasing order of magnitude of charge acquisition. Higher surface energy is correlated to higher negative charge acquisition for $-425+150 \mu\text{m}$ size fraction. Similar trend is also observed with $-150+38 \mu\text{m}$ and $-38 \mu\text{m}$ pyrite size fractions. However, the total surface energy observed after tribo-charging with glass charging medium for $-425+150$, $-150+38$ and $-38 \mu\text{m}$ are 60.60 , 70.18 and 65.33 mJ/m^2 respectively. It is expected that finer fraction

should possess higher surface energy than coarser fraction because of several unsaturated bonds on the surface as the particle size decreases. Inculet *et al.* [22] observed increasing surface energy as the particle size decreases. Lower surface energy for finer size fraction than coarser fraction after tribo-charging with Al, brass and copper is observed. The results distinctly showed a very good correlation between the charge acquisition and surface energy for any of the pyrite size fraction, and higher surface energy corroborates with higher charge acquisition.

The results of total surface energy and its dispersive, polar, acid and base components calculated with van Oss approach are summarised in Table 6. The results in general show that the dispersive component is constant whereas the polar component is decreasing with increasing order of the work function of tribo-charger material. A little deviation in

Table 5. Surface Energy of Pyrites After Tribo-Charging Using with Different Charging Medium Using Fowkes Equation Approach

Particle Size, μm	Charging Medium	Surface Free Energy, mJ/m^2	Disperse Part, mJ/m^2	Polar Part, mJ/m^2
-425+150	Glass	60.60	44.26	16.33
	Aluminium	57.06	44.21	12.85
	Brass	54.70	41.15	13.55
	Copper	44.68	37.95	6.73
-150+38	Glass	70.18	44.27	25.90
	Aluminium	67.63	44.26	23.37
	Brass	64.44	44.21	20.23
	Copper	62.87	44.15	18.72
-38	Glass	65.39	44.16	21.23
	Aluminium	56.15	44.21	11.95
	Brass	53.82	44.14	9.68
	Copper	52.17	44.19	7.98

Table 6. Surface Energy of Pyrite After Tribo-Charging with Different Charging Medium Using van Oss Acid Base Approach

Particle Size, μm	Charging Medium	Surface Free Energy, mJ/m^2	Disperse Part, mJ/m^2	Polar Part, mJ/m^2	Acid Part, mJ/m^2	Base Part, mJ/m^2
-425+150	Glass	54.14	44.18	9.96	1.15	21.57
	Aluminium	53.30	44.13	9.16	1.40	14.96
	Brass	50.85	41.05	9.79	1.61	14.92
	Copper	44.50	37.85	6.65	2.59	4.27
-150+38	Glass	58.28	44.20	14.09	1.36	36.39
	Aluminium	58.36	44.18	14.18	1.62	30.99
	Brass	58.07	44.11	13.96	1.98	24.56
	Copper	57.90	44.05	13.85	2.25	21.33
-38	Glass	58.19	44.08	14.11	1.88	26.51
	Aluminium	55.44	44.09	11.36	3.57	9.02
	Brass	53.65	44.01	9.64	4.16	5.59
	Copper	52.01	44.05	7.96	4.70	3.37

the results in the case of brass for coarser size fraction and aluminium for middle size fraction could be due to the manual tribo-electrification method employed and as well the closeness of work function values among the tribo-charger materials. The effect of tribo-charging on charge acquisition and surface energy is also shown in Figs. (10) and (11). It can be seen from the results in Fig. (10) that the surface energy decreases with increasing order of work function for all size fractions. It can also be observed that the size fractions have higher surface energy when the magnitude of charge on the surface or surface charge density is higher. The higher

surface energy can be correlated to higher electron density on the surface. Although higher magnitude of charge is acquired by $-425+150 \mu\text{m}$ size fraction, its surface energy after tribo-electrification is lower than for $-150+38 \mu\text{m}$ and $-38 \mu\text{m}$ size fractions. The surface energy of $-150+38 \mu\text{m}$ is higher than the $-38 \mu\text{m}$ after contact electrification with all the tribo-charging media except glass where the value remains same at 58 mJ/m^2 . These results suggest that the 40 s time used for tribo-electrification is not sufficient for equilibrium charge development for all the particles in fine size fraction.

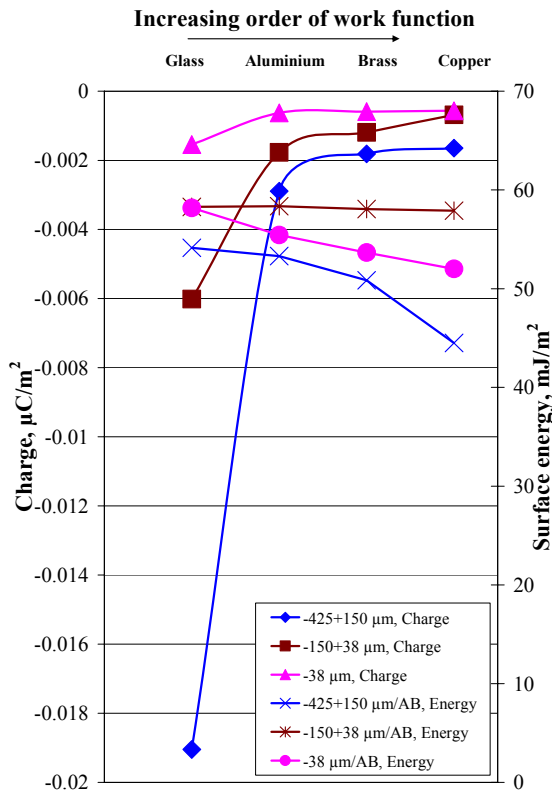


Fig. (10). Effect of tribo-charging on the magnitude of charge acquisition and surface energy using acid-base approach of different pyrite fractions.

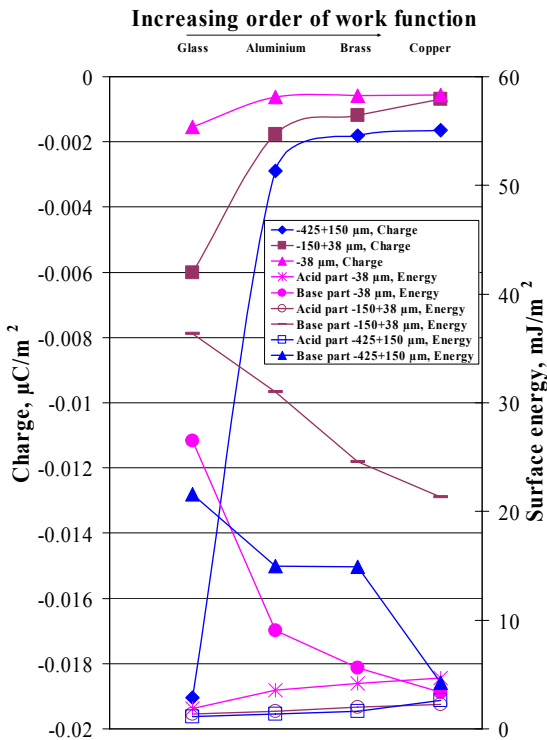


Fig. (11). Effect of tribo-charging on the charge acquisition and acid-base component of different pyrite fractions.

Fig. (11) shows the effect of tribo-charging on charge acquisition and acid-base components of surface energy for the three size fractions. For all size fractions the dispersive component is constant with respect to charging media while the polar part decreases with increasing order of work function of tribo-charger material. The polar part divided into acid and base parts reveals that acid part is increasing while the base part decreasing from glass to copper. The respective acid component after contact electrification with glass, Al, brass and copper for $-425+150 \mu\text{m}$ is 1.15, 1.40, 1.61 and 2.59 mJ/m^2 , for $-150+38 \mu\text{m}$ 1.36, 1.62, 1.98 and 2.25 mJ/m^2 and for $-38 \mu\text{m}$ 1.88, 3.57, 4.16 and 4.70 mJ/m^2 . The acid component suggests the electron acceptance ability of the material. After tribo-electrification pyrite accepted electrons from the charging media and decreased its acidic properties, which suggests the reduction in electron acceptance capability. It can be observed that the higher charge acquisition during tribo-electrification correlates to lowering acid part and increasing base part (Fig. 11). This clearly shows that the base part or electron donating capabilities of pyrite increases after tribo-charging. It can also be observed from Fig. (11) that the acid part for $-425+150$ and $-150+38 \mu\text{m}$ size fractions is lower than for the $-38 \mu\text{m}$ size fraction which explains the condition of equilibrium charging for 40 sec period of contact electrification. The base component of pyrite size fractions also showed that $-150+38 \mu\text{m}$ fraction has higher electron donating capability than $-38 \mu\text{m}$ pyrite fractions. If the $-38 \mu\text{m}$ fraction had attained the equilibrium charging, its acid component could have been lower and the base component could have been higher than the present values.

CONCLUSIONS

The tribo-electrification of different size fractions of pyrite with different tribo-charging media has been carried out and the amount of charge and polarity acquired by the solids are determined by Faraday cup method. All the size fractions charged negatively since they accepted electrons during frictional charging, thus corroborating their higher work function value than the charging medium. The 40 s tribo-charging period is good enough to achieve equilibrium charging for coarser size fractions while the $-38 \mu\text{m}$ fraction needs more time to achieve equilibrium charge density.

The surface characteristics of pyrite fractions after tribo-charging are studied by measuring the polar and non-polar liquid contact angles by Washburn method and calculating the surface energy of solids using well established theoretical approaches. The water contact angle decreases with increasing surface charge density for all the size fractions substantiating electro-wetting phenomena. The higher surface energy corresponded to higher surface charge for all the size fractions and the increase in surface energy follows the order of Cu, brass, Al and glass. The surface energy increases with decreasing particle size. In Fowkes approach, the dispersive part is constant while polar part decreases with decreasing in surface charge density following the work function order.

The van Oss acid-base approach is the most significant approach since the polar part is divided into acid and base components. This approach corroborates with increasing surface energy as the particle size decreases. The dispersive

component is stable while polar part is increasing with decreasing particle size. In all size fractions, the acid part increases and base part decreases with increasing order of work function of tribo-charging media and thus the decreasing order of surface charge acquisition. This explicitly establishes an increase in electron acceptance and decrease in electron donating capabilities of pyrite after tribo-electrification. The respective increase and decrease in acid and base parts followed the work function values of contacting surfaces and consistent with electron transfer from charging medium to pyrite. The findings illustrate a definite correlation between charges generated on powders and acid and base surface energy components calculated from contact angle measurements. The methodology adapted to calculate the surface energy in terms of van Oss acid-base parameters through contact angle measurements is complimentary to the measured surface charge on pyrite particles. The present methodology clarifies the electron transfer mechanism in tribo-electrification and can be used for determining the optimum tribo-charger material. It can also be extended to optimum choice of chemicals (e.g. vapours of acidic and/or basic organic solvents) for enlarging the work function difference in the processing of coal and industrial minerals by tribo-electrostatic method.

ACKNOWLEDGEMENT

The authors gratefully acknowledge the financial support by the Swedish International Development Cooperation Agency (SIDA/SAREC) for the collaboration project, Electrostatic Beneficiation of Indian Thermal Coals.

REFERENCES

- [1] C. Acharya, L.B. Sukla, and V.N. Misra, "Biological elimination of sulphur from high sulphur coal by Aspergillus-like fungi", *Fuel*, vol. 84, pp. 1597-1600, 2005.
- [2] S. Trigwell, K.B. Tennal, and M.K. Mazumder, "Precombustion cleaning of coal by triboelectric separation of minerals", *Particulate Sci. Tech.*, vol. 21, pp. 353-364, 2003.
- [3] E. Nemeth, V. Albrecht, G. Schubert, and F. Simon, "Polymer tribo-electric charging: dependence on thermodynamic surface properties and relative humidity", *J. Electrosta.*, pp. 3-16, 2003
- [4] M.E. Labib, and R. Williams, "The use of zeta-potential measurements in organic solvents to determine the donor-acceptor properties of solid surfaces", *J. Colloid Interface Sci.*, vol. 97, pp. 356-366, 1984.
- [5] M.N. Ahfat, G. Buckton, R. Burrows, and M.D. Ticehurst, "An exploration of inter-relationships between contact angle, inverse phase gas chromatography and triboelectric charging data", *Eur. J. Pharm. Sci.*, vol. 9, pp. 271-276, 2000.
- [6] B. Janczuk, W. Wielslaw, A. Zdziennicka, and F. G. Caballero, "Determination of the galena surface energy components from contact angle measurements", *Mater. Chem. Phys.*, vol. 31, pp. 235-241, 1992.
- [7] C. Karaguzel, M.F. Can, E. Sonmez, and M.S. Celik, "Effect of electrolyte on surface free energy components of feldspar minerals using thin-layer wicking method", *J. Colloid Interface Sci.*, vol. 285, pp. 192-200, 2005.
- [8] M.C. Esposito, S. Chander, and F.F. Aplan, "Characterization of pyrites from coal sources", in A.H. Vassiliou, D.M. Hasen and D.J.T. Carson (Eds.), *Process Mineralogy VII*, TMS, Warrendale, PA, pp. 475-493, 1987.
- [9] W.A. Zisman, "Relation of equilibrium contact angle to liquid and solid constitution", *ACS Adv. Chem. Ser.*, vol. 43, pp. 1-51, 1964.
- [10] F.W. Fowkes, "Determination of interfacial tensions, contact angles, and dispersion forces in surfaces by assuming additivity of intermolecular interactions in surfaces", *J. Phys. Chem.*, Vol. 62, pp. 382-382, 1962.
- [11] F.W. Fowkes, "Attractive forces at interfaces", *Ind. Eng. Chem.*, vol. 56, pp. 40-52, 1964.
- [12] F.M. Fowkes, D.C. McCarthy, and M.A. Mostafa, "Contact angles and the equilibrium spreading pressures of liquids on hydrophobic solids", *J. Coll. Inter. Sci.*, vol. 78, pp. 200-206, 1980.
- [13] C.J. Van Oss, R.J. Good, and M.K. Chaudhury, "The role of van der Waals forces and hydrogen bonds in hydrophobic interactions between biopolymers and low energy surfaces. *J. Colloid Interface Sci.*, vol. 111, pp. 378-390, 1986.
- [14] C.J. van Oss, M.K. Chaudhury, R.J. Good, "Monopolar surfaces", *Adv. Coll. Inter. Sci.*, vol. 28, pp. 35-64, 1987.
- [15] C.J. Oss Van, R.J. Good, and M.K. Chaudhury, "Determination of hydrophobia interaction energy application to separation processes" *Sep. Sci. Tech.* vol. 22, pp. 1-24, 1987.
- [16] W. E. Washburn, "The dynamics of capillary flow", *Phys. Rev.*, vol. 17, 3, pp. 273, 1921.
- [17] S. Trigwell, Dissertation, Dept. of Applied Science, University of Arkansas at Little Rock, AR, USA, 2002.
- [18] H.B. Michaelson, "The work function of the elements and its periodicity", *J. Appl. Phys.*, 48, vol. 11, pp. 4729-4733, 1977.
- [19] I.I. Inculet, "Electrostatic Mineral Separation", Wiley, New York, 1984.
- [20] http://www.siliconfareast.com/tribo_series.htm.
- [21] V.M. Moreno-Villa, M.A. Ponce-Velez, E. Valle-Jaime, and J.L. Fierro-Chavez, "Effect of static charge on hydrophobicity of corona treated glass and silicon rubber surfaces", in Conference record of the 1998 IEEE International Symposium on Electrical Insulation, Arlington, Virginia, USA, June 7-10, 1998, pp. 403-406.
- [22] I.I. Inculet, G.S. Pater Castle, and Gerrit Aartsen, "Generation of bipolar electric fields during industrial handling of powders", *Chem. Engg. Sci.*, vol. 61, pp. 2249-2253, 2006.